frontiers | Frontiers in Surgery

TYPE Original Research
PUBLISHED 12 January 2023
DOI 10.3389/fsurg.2022.1004642

OPEN ACCESS

EDITED BY
Sravisht Iyer,
Hospital for Special Surgery, United States

REVIEWED BY
Yun Peng,
NuVasive (United States), United States
Chen Xu,
Shanghai Changzheng Hospital, China

*CORRESPONDENCE
Jingchi Li
Lijingchi9405@163.com
Ping Cai
Caipingspine@163.com

†These authors have contributed equally to this work and share first authorship

SPECIALTY SECTION
This article was submitted to Orthopedic Surgery, a section of the journal Frontiers in Surgery

RECEIVED 27 July 2022
ACCEPTED 20 September 2022
PUBLISHED 12 January 2023

CITATION
Huang C, Liu Z, Wei Z, Fang Z, Xi Z, Cai P and Li J (2023) Will the adjustment of insertional pedicle screw positions affect the risk of adjacent segment diseases biomechanically? An in-silico study.
Front. Surg. 9:1004642.
doi: 10.3389/fsurg.2022.1004642

Will the adjustment of insertional pedicle screw positions affect the risk of adjacent segment diseases biomechanically? An in-silico study

Chenyi Huang[1†], Zongchao Liu[1†], Zhangchao Wei[1], Zhongxin Fang[2], Zhipeng Xi[3], Ping Cai[4*] and Jingchi Li[1*]

[1]Department of Orthopedics, The Affiliated Traditional Chinese Medicine Hospital of Southwest Medical University, Luzhou, China, [2]Fluid and Power Machinery Key Laboratory of Ministry of Education, Xihua University, Chengdu, China, [3]Department of Spine Surgery, Jiangsu Province Hospital on Integration of Chinese and Western Medicine, Nanjing, China, [4]Department of Orthopedics, Affiliated Hospital of Nanjing University of Chinese Medicine, Nanjing, China

Background: The fixation-induced biomechanical deterioration will increase the risk of adjacent segment diseases (ASD) after lumbar interbody fusion with Bilateral pedicle screw (BPS) fixation. The accurate adjustment of insertional pedicle screw positions is possible, and published studies have reported its mechanical effects. However, no studies clarified that adjusting insertional screw positions would affect the postoperative biomechanical environment and the risk of ASD. The objective of this study was to identify this issue and provide theoretical references for the optimization of insertional pedicle screw position selections.

Methods: The oblique lumbar interbody fusion fixed by BPS with different insertional positions has been simulated in the L4-L5 segment of our previously constructed and validated lumbosacral model. Biomechanical indicators related to ASD have been computed and recorded under flexion, extension, bending, and axial rotation loading conditions.

Results: The change of screw insertional positions has more apparent biomechanical effects on the cranial than the caudal segment. Positive collections can be observed between the reduction of the fixation length and the alleviation of motility compensation and stress concentration on facet cartilages. By contrast, no pronounced tendency of stress distribution on the intervertebral discs can be observed with the change of screw positions.

Conclusions: Reducing the fixation stiffness by adjusting the insertional screw positions could alleviate the biomechanical deterioration and be an effective method to reduce the risk of ASD caused by BPS.

KEYWORDS

adjacent segment diseases, biomechanical deterioration, insertional screw positions, arm of force, pedicle screw fixation

Abbreviations

ASD, Adjacent segment diseases; BEP, Bony endplate; BPS, Bilateral pedicle screw; CBT, Cortical bone trajectory; CEP, Cartilage endplate; DC, Disc compression; FCF, Facet contact force; IDP, Intradiscal pressure; IVD, Intervertebral disc; LIF, Lumbar interbody fusion; OLIF, Oblique lumbar interbody fusion; ROM, Range of motion; ZJ, Zygapophyseal joint.

Introduction

The bilateral pedicle screw (BPS) is extensively used in spinal operations to restore physiological alignment, maintain stability, and correct hypermotility (1, 2). During the lumbar interbody fusion surgery (LIF), BPS could construct three-column instant stability by transpedicular fixation (2, 3). Although BPS is the gold standard of additional fixation technique in LIF surgery, the stiffness-increasing mechanism of BPS will lead to the fixation-induced pathological load transmission pattern (e.g., stress concentration and motility compensation in adjacent segments) and resulting adjacent segment diseases (ASD) (2–4).

Surgeons advocate removing BPS after solid interbody fusion, and its positive biomechanical effects on adjacent segments have been reported by in-silico mechanical simulations (2, 3). But this method has not been widely promoted in clinical practice, for it is difficult for patients without severe symptoms to accept a second surgical trauma. Additionally, low stiffness material connection rods (e.g., Polyether ether ketone rod) have been designed to alleviate postoperative biomechanical deterioration and reduce the risk of ASD. Their biomechanical advantages have also been proved by in-silico and in-vitro mechanical studies (4–8). However, a higher incidence rate of fixator failure and revision surgery inhibits the promotion of these instrumentations (8, 9). Hence, BPS is still the gold standard of the additional fixation device in LIF at the present stage. The optimization of surgical procedures during the use of BPS, rather than the replacement of BPS, may have a better clinical application prospect. During the modification of the screw trajectory, studies reported that the shift of the screw insertion point medially in the coronal plane could alleviate biomechanical deterioration and reduce the risk of ASD (10, 11); the biomechanical mechanism behind the relation between these screw insertion techniques and the risk of ASD should include not only biomechanical changes caused by different grades of the violation of zygapophyseal joints (ZJ) (12, 13), but also the change of fusion segmental stiffness and resulting overall lumbar biomechanical changes (2, 14).

The percutaneous BPS insertion technique is widely promoted (15, 16). Its insertional screw positions can be accurately adjusted under the guidance of the C-arm, but no studies were elucidating the biomechanical changes with the adjustment of screw insertion positions in the sagittal plane. Adjusting screw insertion positions will affect the BPS's fixation length and locally biomechanical impacts on adjacent segments (2, 14). Considering long segment LIF with the expansion of fixation length has been proven a risk factor of ASD (17, 18), we believe that optimizing screw insertion positions in the sagittal plane (i.e., reducing the fixation length) may be an effective method to reduce the risk of ASD biomechanically. The objective of this study was to identify the biomechanical significance of insertional pedicle screw positions on the risk of ASD. Published literature has not adequately clarified this issue to the best of our knowledge.

Methods

Model construction

We simulate oblique lumbar interbody fusion (OLIF) fixed by BPS with different insertional positions in a previously constructed and well-validated lumbosacral model (19, 20). Bone structures include cortical, cancellous, and bony endplates (BEP), the thickness and morphology of BEPs were defined according to the measurement of large sample imaging data (21, 22). Nonbony components include the intervertebral disc (IVD) and ZJ cartilages. IVD consists of the nucleus core, the surrounding annulus, and cartilage endplates (CEP) on the cranial and caudal sides of the nucleus and inner part of the annulus (23, 24).

Boundary and loading conditions

Models were computed under identical loading conditions, including flexion, extension, bending, and rotation. Sizes of the moment in the mechanical indicators computation process were consistent with the validation of the range of motion (ROM). They were set to be symmetric in the sagittal plane to increase their computational efficiency by allowing the unilateral calculation of the bending and axial rotation loading conditions (19, 20). Hybrid elements (including tetrahedron and hexahedron) with different mesh sizes were established in different components, and smaller mesh sizes were used in structures with low thickness and large deformation (20, 25).

In the definition of material properties, cortical and cancellous bone were set as anisotropic materials (26, 27), other parts of the model were defined by isotropic law (26, 27). The annulus was assumed to be hypoelastic (26, 28), and the nucleus was set as an incompressible "semi-fluid pad" (25, 29). Ligaments structures and capsules of ZJ were defined as cable elements in the pre-processing step of FEA (**Table 1**) (25, 29–31). Contact elements defined facet cartilages of ZJ, and its frictional coefficient was set as zero (29, 32).

Model calibration and validation

All freedom degrees were fixed under the inferior surfaces of current models, and moments were applied on their superior surfaces (5, 29). The stiffness of ligaments under different loading conditions was calibrated to reduce the difference

TABLE 1 Material properties of components in current models.

Components	Elastic modulus (MPa)	Poisson's ratio	Cross-section (mm^2)
Cortical	E_{xx} = 11,300 E_{yy} = 11,300 E_{zz} = 22,000 G_{xy} = 3,800 G_{yz} = 5,400 G_{xz} = 5,400	V_{xy} = 0.484 V_{yz} = 0.203 V_{xz} = 0.203	/
Cancellous	E_{xx} = 140 E_{yy} = 140 E_{zz} = 200 G_{xy} = 48.3 G_{yz} = 48.3 G_{xz} = 48.3	V_{xy} = 0.45 V_{yz} = 0.315 V_{xz} = 0.315	/
Bony endplates	12,000	0.3	/
Annulus	Hypoelastic material		/
Nucleus	1	0.49	/
Cartilage endplates	10	0.4	/
Anterior longitudinal ligaments	Calibrated load-deformation curved under different loading conditions	0.3	60
Posterior longitudinal ligaments	Calibrated load-deformation curved under different loading conditions	0.3	21
Ligamentum flavum	Calibrated load-deformation curved under different loading conditions	0.3	60
Interspinous ligaments	Calibrated load-deformation curved under different loading conditions	0.3	40
Supraspinous ligaments	Calibrated load-deformation curved under different loading conditions	0.3	30
Intertransverse ligaments	Calibrated load-deformation curved under different loading conditions	0.3	10
Capsular	7.5 (\25%) 32.9 ([25%)	0.3	67.5
PEEK	3,500	0.3	/
Titanium alloy	110,000	0.3	/

between the computed ROM in the L4-L5 segment and in-vitro studies (33, 34). A mesh convergency test on the intact model was performed by evaluating intradiscal pressure (IDP) change with different mesh sizes. The model was considered converged if the change of computed IDP was less than 3% (35, 36), multi-indicators model validation has been accomplished by comparing the computed ROM, IDP, the disc compression (DC), and the facet contact force with values from in-vitro studies under different sizes and directions load to ensure computational credibility (37, 38).

Surgical simulations and ASD's risk evaluation

The L4-L5 segment has been selected to simulate the oblique lumbar interbody fusion (OLIF) fixed by BPS with different insertional positions for the incidence rate of lumbar degenerative diseases in this segment was higher than that of the L3-L4 segment, and the L5-S1 segment was not suitable for OLIF generally (15, 16). Lateral parts of the annulus, all of the nucleus, and CEPs in the surgical segment were removed, and a PEEK OLIF cage (18 mm long and 50 mm wide) filled with grafted bony material was inserted into interbody space (15, 39). It was assumed that the disc height and lordotic angle of disc space were not affected by cage insertion, and the outline between cage and BEP was assumed to be perfectly matched (3, 30, 40). Considering ASD was a typical long-term complication, the boundary conditions have been defined to simulate solid interbody fusion. In which, the contact type between grafted bone and BEP was set to be "bounded" (completely constrains the motion under all degrees of freedom), and the frictional coefficient in surfaces between cage and BEP was 0.8 (41, 42).

During the simulation of titanium alloy (Ti6Al4V) BPS fixation with different insertion positions, bilateral pedicle screws (were inserted into L4 and L5 vertebral bodies. The axes of screws on the cross-section were parallel to the pedicle axis, and the screw axis was parallel to which of corresponding cranial BEP (5, 16). The connection between the screw tulip and the nut was simplified to reduce the computational burden (2, 5). Five postoperative models with different insertional screw positions have been constructed, and the screw compaction effect was simulated by adjusting the material property of bony tissue around the screw thread (43, 44). Motility parameters, stress distribution in IVD, and ZJ in both cranial and caudal sides of functional units were recorded to evaluate the risk of ASD.

Results

Multi-indicators model validation

Well-validated computational results can be recorded in the intact model. Specifically, the values of computed ROM and DC under were compared with which in in-vitro studies reported by Renner et al (38), values of IDP were compared with the study published by Schilling et al (7), and which of FCF were also compared with Wilson et al.'s study (37). These indicators computed by the intact model were within ±1 standard deviation of the average values reported by the above-mentioned in-vitro studies, proving that current models could make a good representation of real biomechanical situations (**Figure 1**).

Changes in mechanical indicators related to ASD

Overall ROM, ROM in different segments (including the surgical and adjacent segments), and the proportion of different segmental ROM to the overall value have been computed and recorded to evaluate the motility compensation. Except for the axial rotation condition, positive relations between BPS's fixation length and fixational stiffness can be observed. Specifically, the change of fixation length will slightly affect the overall ROM (the variation range was smaller than 5% except for model 2 (model with shortest fixation length) under the flexion loading condition). By contrast, the change of ROM in the fusion segment was dramatically under most loading conditions. Meanwhile, pathological motility compensation could be amplified and alleviated by increasing and decreasing the arm of force in these segments, especially under the flexion condition in the cranial and bending in the caudal segment (**Figures 2**, **3**).

FCF was not recorded under the flexion loading condition for ZJ cartilages that were not in contact. For the same reason, FCF on the opposite side to the bending condition and the rotation side could not be recorded. In other words, FCF under left lateral bending is observed on left-side cartilages, while FCF under left axial rotation is observed on right-side cartilages. The change of insertional screw positions can lead to the change of FCF. Generally, reducing the arm of force in adjacent segments will decrease FCF and vice versa (**Figure 4**). The variation tendency of the cranial side was more pronounced than the caudal one. To investigate the risk of disc degeneration, we calculate IDP, maximum values of annulus shear and equivalent stress (**Figure 5**). Inconsistent with the variation tendency of ROM and FCF, no apparent tendency of these mechanical indicators can be observed with the change of insertional screw positions, especially under the rotation condition.

Discussion

This work evaluated biomechanical deterioration and the related risk of ASD after OLIF fixed by BPS with different insertional screw positions. An intact lumbosacral model and corresponding OLIF models were constructed, and biomechanical indicators closely related to ASD were computed and evaluated. The importance of the biomechanical environment for achieving positive postoperative clinical outcomes has been repeatedly demonstrated (2, 17, 29). Thus, investigations on the biomechanical effects of different insertional screw positions are of great significance for optimal operative strategy and reducing the risk of ASD.

OLIF, rather than other LIF operations, has been selected for the following reasons. The percutaneous pedicle screw insertion was accomplished under C-arm fluoroscopy in OLIF, and the adjustment of insertion positions is feasible in this operation (**Figure 6**). By contrast, selecting screw insertion positions in other lumbar fusion operations (e.g., transforaminal and posterior lumbar interbody fusion) was based on identifying anatomic structures (10, 11). Considering the prevalence of anatomic variations and the hypertrophy of the articular process during the pathological process of spinal stenosis (45, 46), it is difficult to accurately judge and adjust the exact insertional screw position under the freehand pedicle insertion process. Furthermore, for the same reason, the promotion of the optimized insertional screw positions elucidated by this study may also be limited in LIF fixed by percutaneous pedicle screw.

The deterioration of the biomechanical environment caused by inappropriate surgery may be continuously amplified and lead to a devastating prognosis (17, 19, 47). Therefore, optimizing a surgical technique based on a biomechanical study is significant. There are three common pathological changes of ASD: disc degeneration, ZJ degenerative osteoarthritis, spinal stenosis, and segmental instability (17, 48). The annulus-driven phenotype is the most common reason for disc degeneration in the lower lumbar spine (49, 50). Stress concentration on the annulus, especially on the post and post-lateral parts of the annulus, were related to different types of annulus tears (34, 51). Meanwhile, the aberrant increase of IDP could also increase the risk of annulus failure (26, 52); therefore, annulus stress distribution and IDP are critical indicators in related mechanical studies (26, 53). Simultaneously annulus tears and increased intradiscal pressure would promote disc herniation. The in-growth of blood vessels along annulus tears will promote the inflammatory response, leading to extracellular matrix catabolism and further disc degeneration (50, 54). The in-growth of pain-sensing nerve fibers is also the primary reason for postoperative pain recurrence in ASD (54, 55).

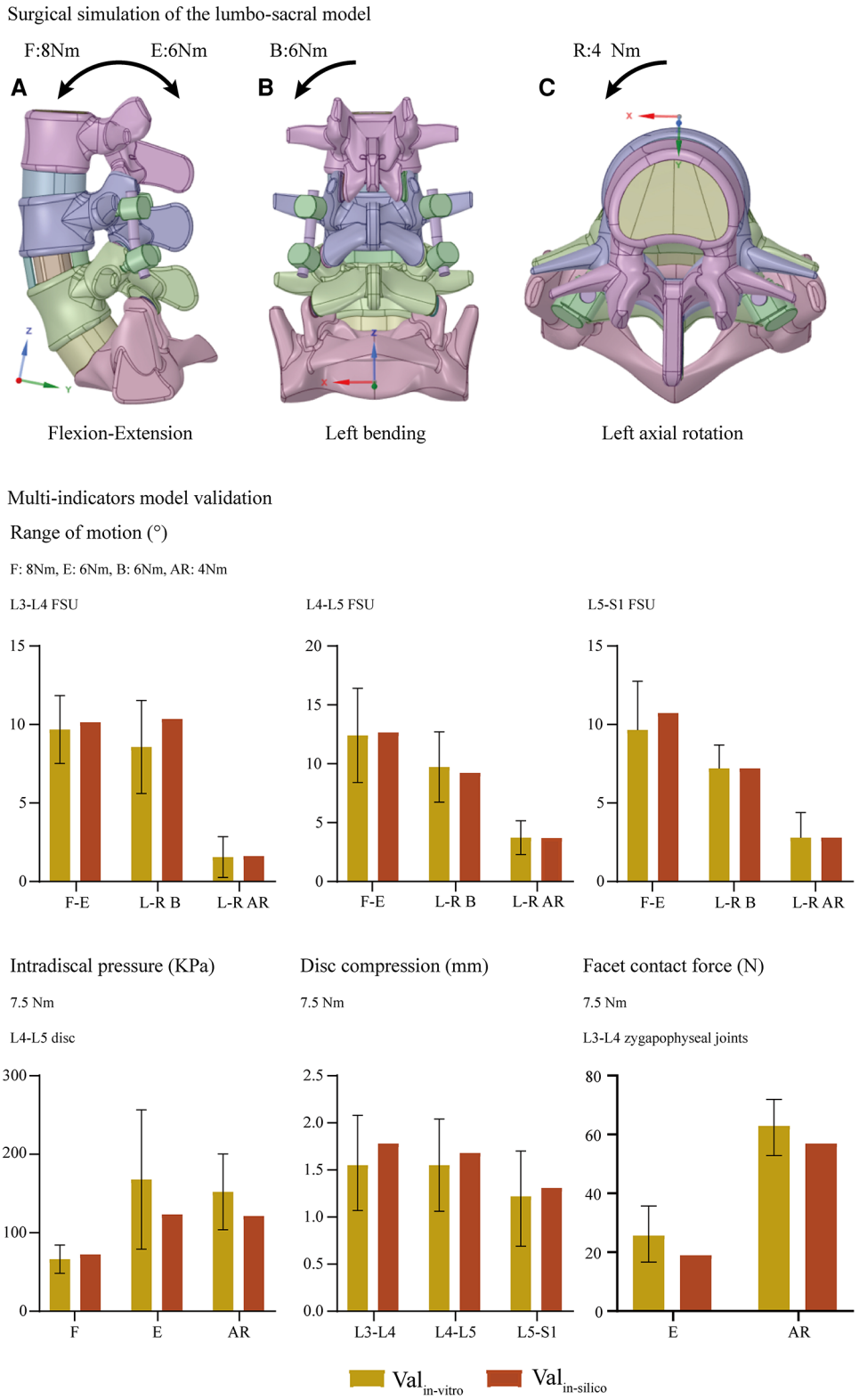

FIGURE 1
Surgical simulations and multi indicators model validation: $Val_{in-vitro}$, indicators measured by published in-vitro studies; $Val_{in-silico}$, indicators computed by the current in-silico study; F-E, flexion-extension; L-R, left-lateral; B, bending; AR, axial rotation.

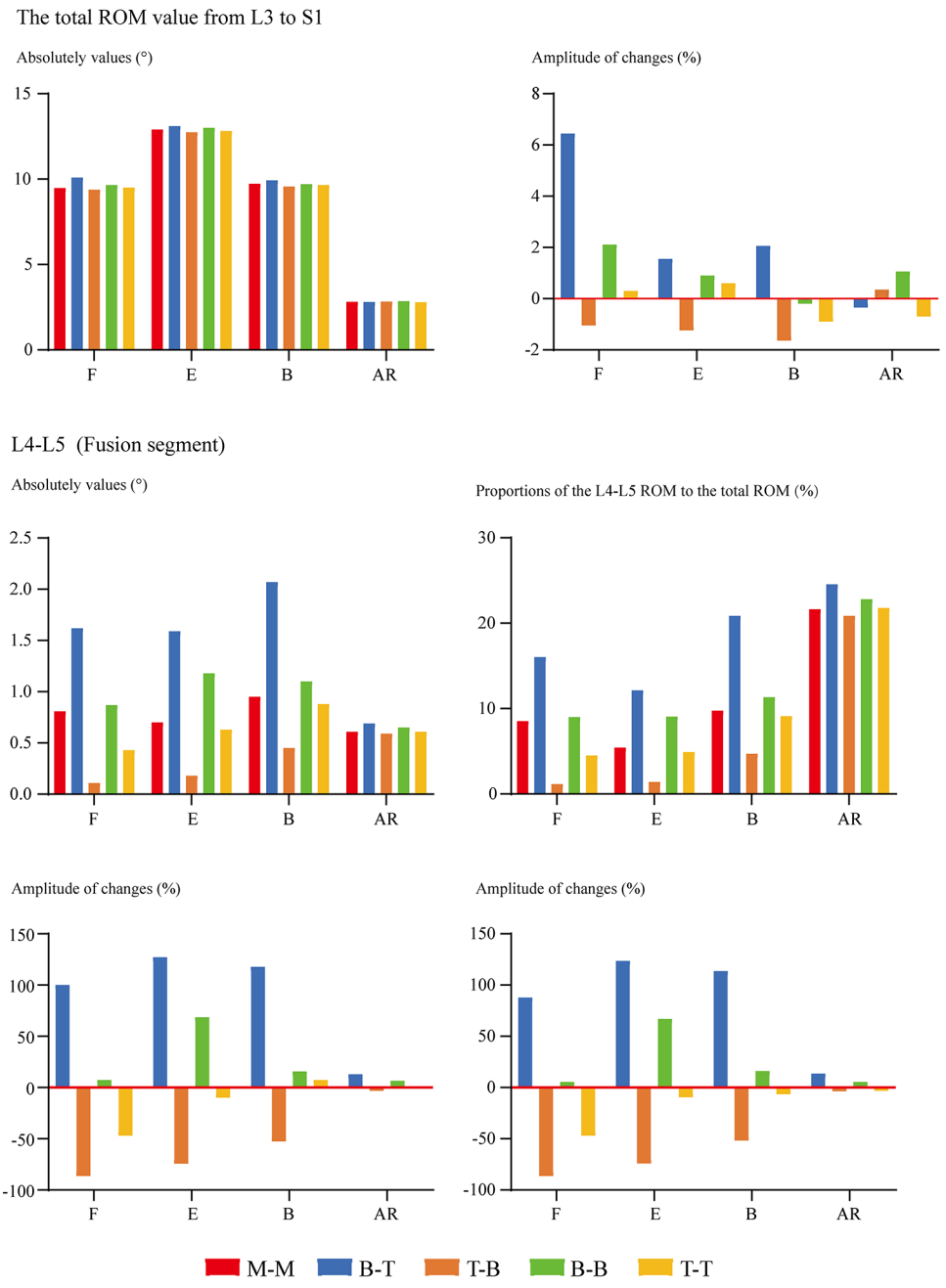

FIGURE 2
Comparison of overall and surgical segment's ROM between surgical models with different insertional screw positions. F, Flexion; E, Extension; B, Bending; AR, Axial rotation.

The pathological change in ASD was not limited to IVD. The degenerative osteoarthritis, hypertrophy of the articular process, and resulting spinal canal stenosis were also essential triggers symptoms recurrence (42, 56). Therefore, ZJ degeneration should also be considered in ASD, which can be well reflected by evaluating the FCF (19, 26) Additionally, as mentioned above, postoperative pathological motility compensation and resulting spinal instability is also a basic form of ASD (17, 42), which could be reflected by the variation of ROM and its proportion (5, 47). Therefore, ROM can be used as an indicator for model calibration and validation, and assess ASD's risk. Moreover, the interaction between segmental instability and spinal canal stenosis was also clearly elucidated, reactive hyperplasia of the articular process and ligamentum structures caused by segmental instability was the main reason for spinal stenosis over a long

10.3389/fsurg.2022.1004642

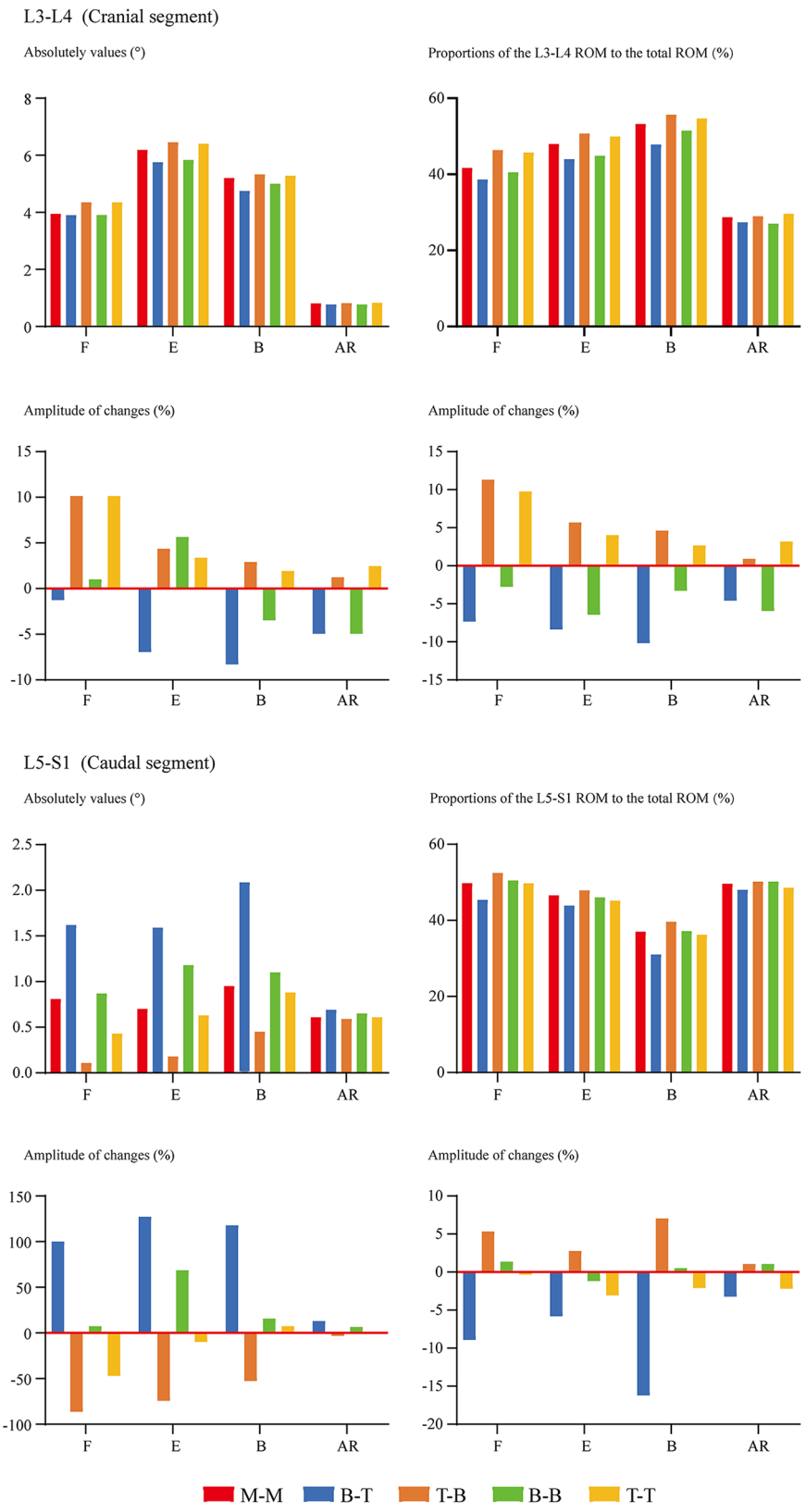

FIGURE 3
Comparison of cranial and caudal adjacent segments' ROM between surgical models with different insertional screw positions. F, Flexion; E, Extension; B, Bending; AR, Axial rotation.

10.3389/fsurg.2022.1004642

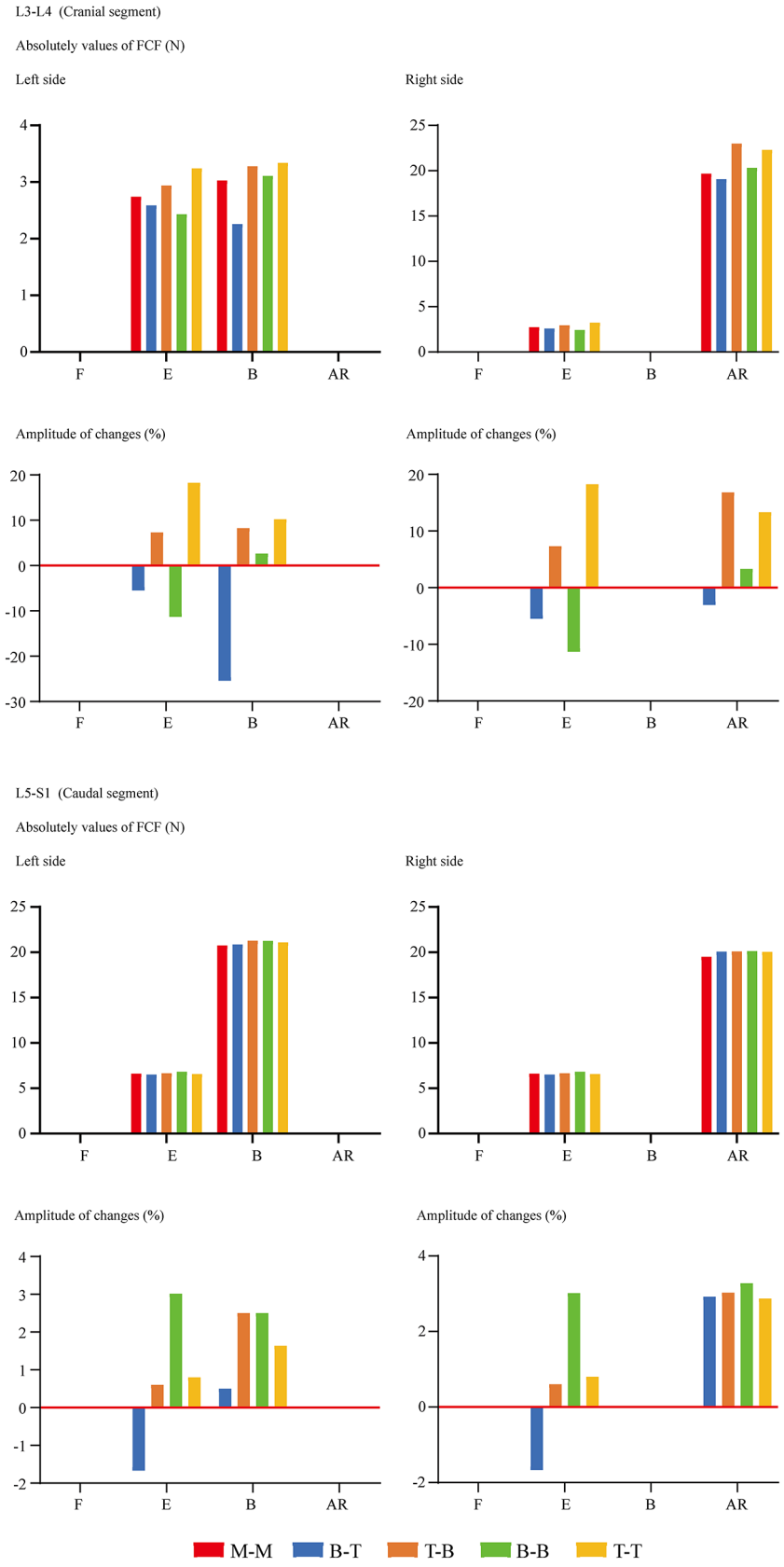

FIGURE 4
Comparison of FCF between surgical models with different insertional screw positions. F, Flexion; E, Extension; B, Bending; AR, Axial rotation.

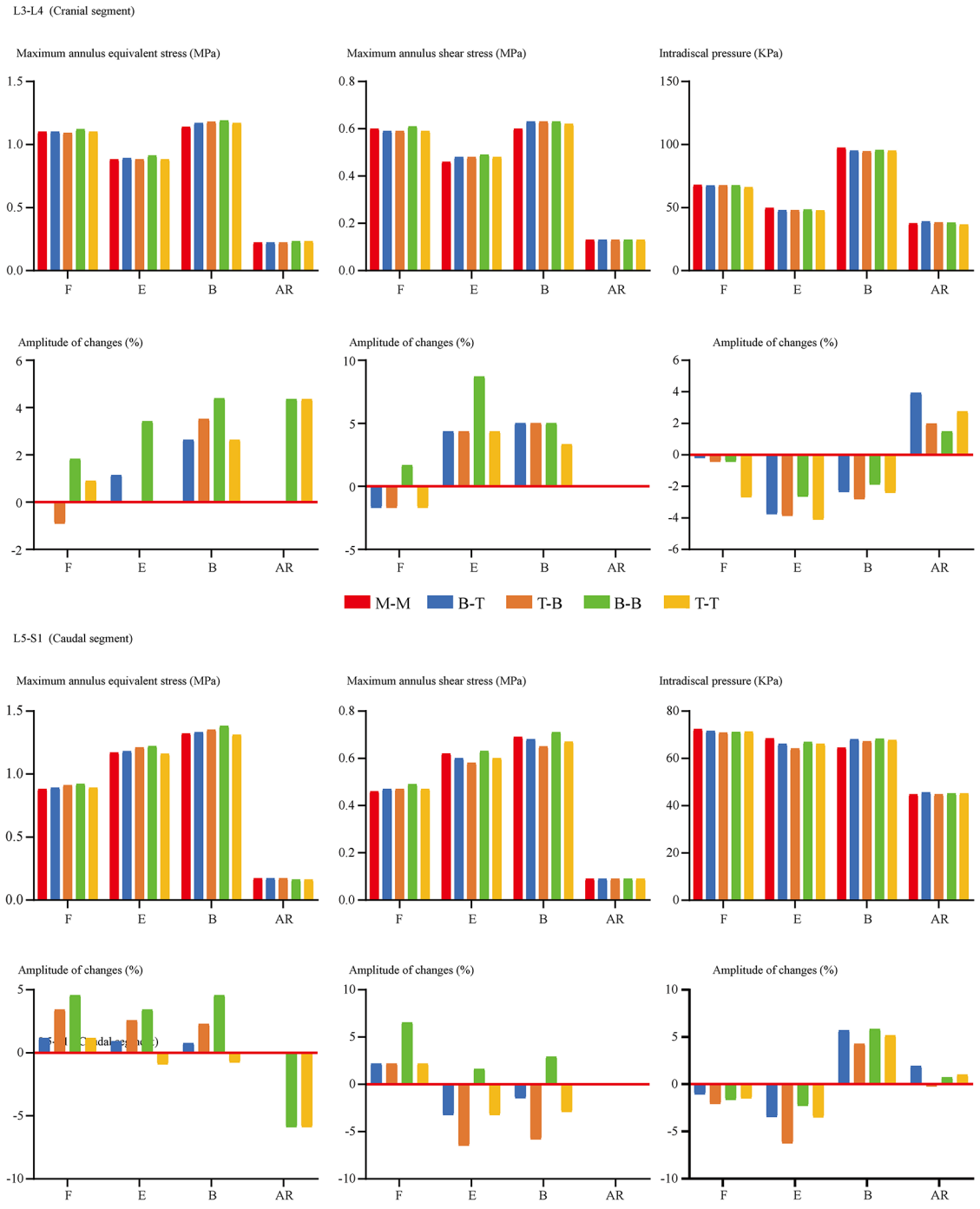

FIGURE 5
Comparison of indicators related to the cranial and caudal disc degeneration between surgical models with different insertional screw positions. F, Flexion; E, Extension; B, Bending; AR, Axial rotation.

period (45, 57). In a word, by computing these biomechanical indicators, the risk of ASD could be investigated systematically.

Based on the current computational results, slight changes in stress concentration on the disc can be observed in cranial and caudal IVDs. Therefore, we can deduce that the tendency of disc degeneration acceleration may not be changed obviously with the change of arm of force. By contrast, the fixation stiffness in the surgical segment and motility compensation in adjacent segments could be distinctly affected by the change of fixation length. Pronounced motility

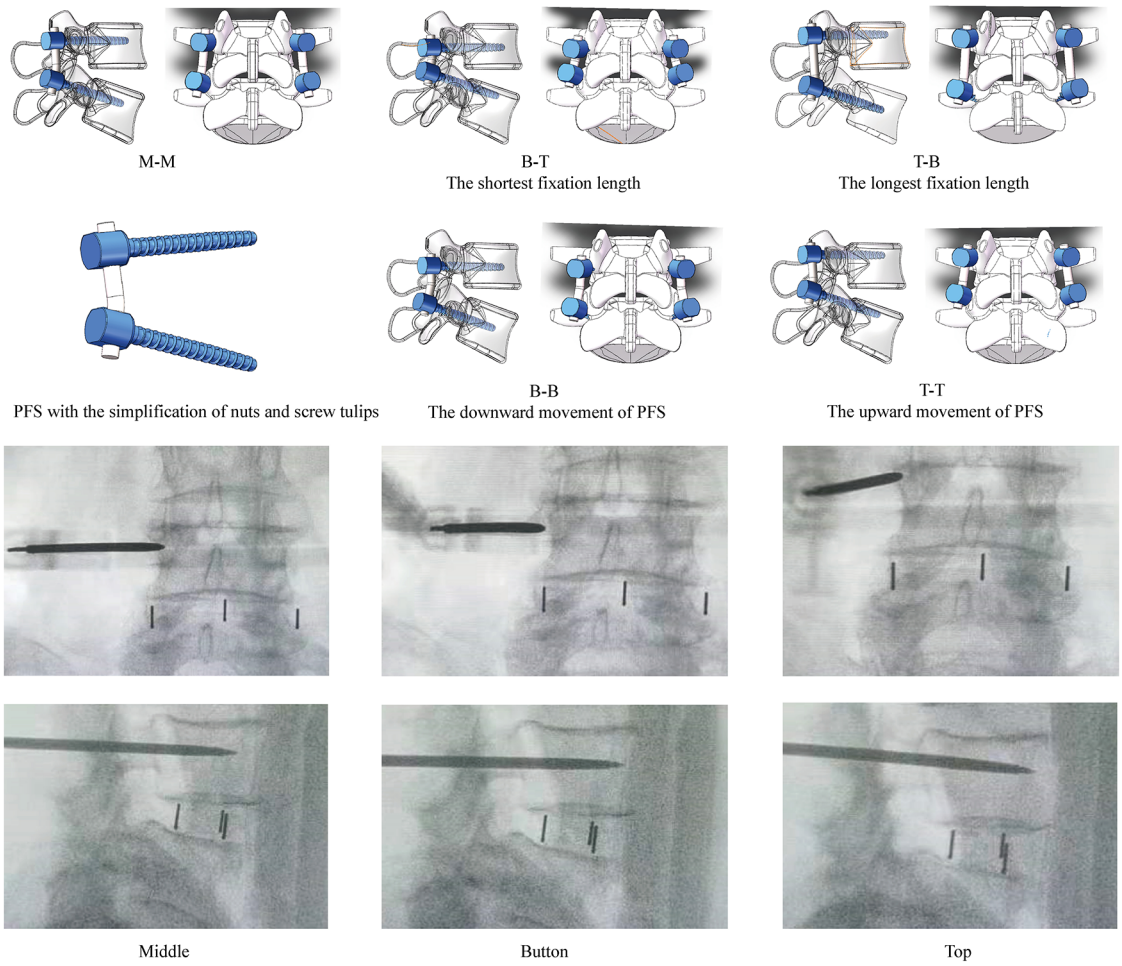

FIGURE 6
Diagrams of OLIF fixed by PFS with different insertional screw positions, and the highly adjustable of percutaneous BPS insertion. M-M: Screws were inserted into the middle positions of both cranial and caudal vertebral bodies; B-T: Screws were inserted into the bottom of the cranial and the top of the caudal vertebral bodies (Shortest fixation length of PFS); T-B: Screws were inserted into the top of the cranial and the bottom of the caudal vertebral bodies (Longest fixation length of PFS); BB: Screws were inserted into the bottom of both cranial and caudal vertebral bodies (The downward movement of PFS); TT: Screws were inserted into the top of both cranial and caudal vertebral bodies (The upward movement of PFS).

compensation can be recorded when the fixation length increases and the BPS shift towards the measured side. Meanwhile, although the range of variations is higher in the cranial than the caudal segment, the overall variation tendency of FCF is still consistent with which of the motility compensation. Considering above mentioned interaction between segmental instability and spinal canal stenosis (45, 57), the reduction of BPS's fixation length by adjusting the percutaneous BPS's positions could optimize the local biomechanical environment and reduce the risk of adjacent segmental instability in the short term and spinal stenosis in the long term in both cranial and caudal motion segments adjacent to the surgical segment with percutaneous BPS fixation.

Admittedly, the current study results should be interpreted within the context of the following-mentioned limitations. Firstly, the mechanical effect of ligaments can only be acted on artificially selected positions rather than their entire original surfaces. We defined these ligaments as cable elements, and the potential risk of mechanical indicators distortions should be considered. However, we believe that the computational results elucidated by current models are still reliable for the following reasons. The definition of cable ligaments has been widely used in the same kind of in-silico spinal studies (25, 29, 51), and the multi-indicators model validation has guaranteed the credibility of the current models. Additionally, no attach positions of cable elements are defined on structures with computed indicators (e.g., annulus, CEPs, and facet cartilages of ZJ); this determines that even if there is computational distortion, it can be excluded from the indicator's computation. The definition of ligaments should still be optimized in future in-silico studies. Meanwhile, the damage to facet joint capsule and facet cartilages were not

simulated in this study. That's because current FEA studies never research this topic, so it is not easy to find a widely accepted standard to simulate this topic in our models. But the simulation of this topic may be necessary and should be performed in our future studies. Moreover, we could not provide clinical evidence to verify the computed biomechanical changes in the current study. We admit that corresponding clinical evidence is of great significance to this topic, and we will try to provide clinical evidence in our future studies.

Conclusion

Collectively, computed indicators in this study elucidated that during LIF operations fixed by percutaneous BPS, reducing the fixation stiffness by adjusting the insertional screw positions on the sagittal plane could alleviate motility compensation and stress concentration on ZJ cartilages, especially on the cranial segment. Thus, this mechanical effect may be an effective method to reduce the risk of ASD (adjacent segmental instability in the short term and spinal stenosis in the long term).

Data availability statement

The original contributions presented in the study are included in the article/Supplementary Material, further inquiries can be directed to the corresponding author/s.

Ethics statement

The studies involving human participants were reviewed and approved by Approval for the current study protocol (including the lumbar CT scan) was obtained from the ethics committees of Jiangsu Province Hospital on Integration of Chinese and Western Medicine (2019LWKY015). We confirm that the subject signed the informed consent and submitted it to the ethics committee for review before the examination, and all methods were carried out in accordance with relevant guidelines and regulations.. Written informed consent for participation was not required for this study in accordance with the national legislation and the institutional requirements.

Author contributions

Conception and design: JL, PC, and CH; Model construction and finite element analysis: JL, ZF and PC; Analysis and interpretation of data: CH, ZL and JL; Figures preparation: CH, ZW, ZF, and ZX; Manuscript Preparation and modification: CYH, ZL, PC and JL. All authors contributed to the article and approved the submitted version.

Funding

This study was supported by the project of applied basic research in the Southwest Medical University (2021ZKQN129) and the Hejiang County People's Hospital - Southwest Medical University Cooperative project (2021HJXNYD08).

Acknowledgments

We acknowledge Mr. Xiaoyu Zhang for the guidance of figures drawing.

Conflict of interest

The authors declare that the research was conducted in the absence of any commercial or financial relationships that could be construed as a potential conflict of interest.

Publisher's note

References

1. Xu M, Yang J, Lieberman IH, Haddas R. Finite element method-based study of pedicle screw-bone connection in pullout test and physiological spinal loads. *Med Eng Phys*. (2019) 67:11–21. doi: 10.1016/j.medengphy.2019.03.004

2. Hsieh YY, Chen CH, Tsuang FY, Wu LC, Lin SC, Chiang CJ. Removal of fixation construct could mitigate adjacent segment stress after lumbosacral fusion: a finite element analysis. *Clin Biomech (Bristol Avon)*. (2017) 43:115–20. doi: 10.1016/j.clinbiomech.2017.02.011

3. Tsuang FY, Tsai JC, Lai DM. Effect of lordosis on adjacent levels after lumbar interbody fusion, before and after removal of the spinal fixator: a finite element analysis. *BMC Musculoskelet Disord*. (2019) 20(1):470. doi: 10.1186/s12891-019-2886-4.

4. Galbusera F, Bellini CM, Anasetti F, Ciavarro C, Lovi A, Brayda-Bruno M. Rigid and flexible spinal stabilization devices: a biomechanical comparison. *Med Eng Phys*. (2011) 33(4):490–6. doi: 10.1016/j.medengphy.2010.11.018

5. Chuang WH, Lin SC, Chen SH, Wang CW, Tsai WC, Chen YJ, et al. Biomechanical effects of disc degeneration and hybrid fixation on the transition and adjacent lumbar segments: trade-off between junctional problem, motion preservation, and load protection. *Spine*. (2012) 37(24):E1488–97. doi: 10.1097/BRS.0b013e31826cdd93

6. Hsieh YY, Tsuang FY, Kuo YJ, Chen CH, Chiang CJ, Lin CL. Biomechanical analysis of single-level interbody fusion with different internal fixation rod materials: a finite element analysis. *BMC Musculoskelet Disord*. (2020) 21(1):100. doi: 10.1186/s12891-020-3111-1

7. Schilling C, Krüger S, Grupp TM, Duda GN, Blömer W, Rohlmann A. The effect of design parameters of dynamic pedicle screw systems on kinematics and load bearing: an in vitro study. *Eur Spine J*. (2011) 20(2):297–307. doi: 10.1007/s00586-010-1620-6

8. Lee MJ, Lindsey JD, Bransford RJ. Pedicle screw-based posterior dynamic stabilization in the lumbar spine. *J Am Acad Orthop Surg*. (2010) 18(10):581–8. doi: 10.5435/00124635-201010000-00001

9. Lee CH, Kim YE, Lee HJ, Kim DG, Kim CH. Biomechanical effects of hybrid stabilization on the risk of proximal adjacent-segment degeneration following lumbar spinal fusion using an interspinous device or a pedicle screw-based dynamic fixator. *J Neurosurg Spine*. (2017) 27(6):643–9. doi: 10.3171/2017.3.Spine161169

10. He B, Yan L, Guo H, Liu T, Wang X, Hao D. The difference in superior adjacent segment pathology after lumbar posterolateral fusion by using 2 different pedicle screw insertion techniques in 9-year minimum follow-up. *Spine*. (2014) 39(14):1093–8. doi: 10.1097/brs.0000000000000353

11. Kim HJ, Chun HJ, Kang KT, Moon SH, Kim HS, Park JO, et al. The biomechanical effect of pedicle screws' insertion angle and position on the superior adjacent segment in 1 segment lumbar fusion. *Spine*. (2012) 37(19):1637–44. doi: 10.1097/BRS.0b013e31823f2115

12. Li J, Li H, He Y, Zhang X, Xi Z, Wang G, et al. The protection of superior articular process in percutaneous transforaminal endoscopic discectomy should decreases the risk of adjacent segment diseases biomechanically. *J Clin Neurosci*. (2020) 79:54–9. doi: 10.1016/j.jocn.2020.07.025

13. Cardoso MJ, Dmitriev AE, Helgeson M, Lehman RA, Kuklo TR, Rosner MK. Does superior-segment facet violation or laminectomy destabilize the adjacent level in lumbar transpedicular fixation? An in vitro human cadaveric assessment. *Spine*. (2008) 33(26):2868–73. doi: 10.1097/BRS.0b013e31818c63d3

14. La Barbera L, Costa F, Villa T. ISO 12189 Standard for the preclinical evaluation of posterior spinal stabilization devices–II: a parametric comparative study. Proceedings of the institution of mechanical engineers part H. *J Eng Med*. (2016) 230(2):134–44. doi: 10.1177/0954411915621588

15. Guo HZ, Tang YC, Guo DQ, Luo PJ, Li YX, Mo GY, et al. Stability evaluation of oblique lumbar interbody fusion constructs with Various fixation options: a finite element analysis based on three-dimensional scanning models. *World Neurosurg*. (2020) 138:e530–8. doi: 10.1016/j.wneu.2020.02.180

16. Quillo-Olvera J, Lin GX, Jo HJ, Kim JS. Complications on minimally invasive oblique lumbar interbody fusion at L2-L5 levels: a review of the literature and surgical strategies. *Ann Transl Med*. (2018) 6(6):101. doi: 10.21037/atm.2018.01.22

17. Wang H, Ma L, Yang D, Wang T, Liu S, Yang S, et al. Incidence and risk factors of adjacent segment disease following posterior decompression and instrumented fusion for degenerative lumbar disorders. *Med (Baltimore)*. (2017) 96(5):e6032. doi: 10.1097/md.0000000000006032

18. Park P, Garton HJ, Gala VC, Hoff JT, McGillicuddy JE. Adjacent segment disease after lumbar or lumbosacral fusion: review of the literature. *Spine*. (2004) 29(17):1938–44. doi: 10.1097/01.brs.0000137069.88904.03

19. Li J, Xu C, Zhang X, Xi Z, Liu M, Fang Z, et al. TELD With limited foraminoplasty has potential biomechanical advantages over TELD with large annuloplasty: an in-silico study. *BMC Musculoskelet Disord*. (2021) 22(1):616. doi: 10.1186/s12891-021-04504-1

20. Li J, Xu C, Zhang X, Xi Z, Sun S, Zhang K, et al. Disc measurement and nucleus calibration in a smoothened lumbar model increases the accuracy and efficiency of in-silico study. *J Orthop Surg Res*. (2021) 16(1):498. doi: 10.1186/s13018-021-02655-4

21. Liu JT, Han H, Gao ZC, He CY, Cai X, Niu BB, et al. [CT assisted morphological study of lumbar endplate]. *Zhongguo Gu Shang*. (2018) 31(12):1129–35. doi: 10.3969/j.issn.1003-0034.2018.12.011

22. Pan CL, Zhang BY, Zhu YH, Ma YH, Li MF, Wang X, et al. Morphologic analysis of Chinese lumbar endplate by three-dimensional computed tomography reconstructions for helping design lumbar disc prosthesis. *Med (Baltimore)*. (2021) 100(6):e24583. doi: 10.1097/md.0000000000024583

23. DeLucca JF, Cortes DH, Jacobs NT, Vresilovic EJ, Duncan RL, Elliott DM. Human cartilage endplate permeability varies with degeneration and intervertebral disc site. *J Biomech*. (2016) 49(4):550–7. doi: 10.1016/j.jbiomech.2016.01.007

24. Jacobs NT, Cortes DH, Peloquin JM, Vresilovic EJ, Elliott DM. Validation and application of an intervertebral disc finite element model utilizing independently constructed tissue-level constitutive formulations that are nonlinear, anisotropic, and time-dependent. *J Biomech*. (2014) 47(11):2540–6. doi: 10.1016/j.jbiomech.2014.06.008

25. Dreischarf M, Zander T, Shirazi-Adl A, Puttlitz CM, Adam CJ, Chen CS, et al. Comparison of eight published static finite element models of the intact lumbar spine: predictive power of models improves when combined together. *J Biomech*. (2014) 47(8):1757–66. doi: 10.1016/j.jbiomech.2014.04.002

26. Tsouknidas A, Sarigiannidis SO, Anagnostidis K, Michailidis N, Ahuja S. Assessment of stress patterns on a spinal motion segment in healthy versus osteoporotic bony models with or without disc degeneration: a finite element analysis. *Spine J*. (2015) 15(3 Suppl):S17–s22. doi: 10.1016/j.spinee.2014.12.148

27. !!! INVALID CITATION !!! {}.

28. Wu HC, Yao RF. Mechanical behavior of the human annulus fibrosus. *J Biomech*. (1976) 9(1):1–7. doi: 10.1016/0021-9290(76)90132-9

29. Chuang WH, Kuo YJ, Lin SC, Wang CW, Chen SH, Chen YJ, et al. Comparison among load-, ROM-, and displacement-controlled methods used in the lumbosacral nonlinear finite-element analysis. *Spine*. (2013) 38(5):E276–85. doi: 10.1097/BRS.0b013e31828251f9

30. Zhou C, Cha T, Wang W, Guo R, Li G. Investigation of alterations in the lumbar disc biomechanics at the adjacent segments after spinal fusion using a combined in vivo and in silico approach. *Ann Biomed Eng*. (2021) 49(2):601–16. doi: 10.1007/s10439-020-02588-9

31. Zhou C, Cha T, Li G. An upper bound computational model for investigation of fusion effects on adjacent segment biomechanics of the lumbar spine. *Comput Methods Biomech Biomed Engin*. (2019) 22(14):1126–34. doi: 10.1080/10255842.2019.1639047

32. Woldtvedt DJ, Womack W, Gadomski BC, Schuldt D, Puttlitz CM. Finite element lumbar spine facet contact parameter predictions are affected by the cartilage thickness distribution and initial joint gap size. *J Biomech Eng*. (2011) 133(6):061009. doi: 10.1115/1.4004287

33. Schmidt H, Heuer F, Simon U, Kettler A, Rohlmann A, Claes L, et al. Application of a new calibration method for a three-dimensional finite element model of a human lumbar annulus fibrosus. *Clin Biomech (Bristol Avon)*. (2006) 21(4):337–44. doi: 10.1016/j.clinbiomech.2005.12.001

34. Schmidt H, Heuer F, Drumm J, Klezl Z, Claes L, Wilke HJ. Application of a calibration method provides more realistic results for a finite element model of a lumbar spinal segment. *Clin Biomech (Bristol Avon)*. (2007) 22(4):377–84. doi: 10.1016/j.clinbiomech.2006.11.008

35. Fan W, Guo LX, Zhang M. Biomechanical analysis of lumbar interbody fusion supplemented with various posterior stabilization systems. *Eur Spine J*. (2021) 30(8):2342–50. doi: 10.1007/s00586-021-06856-7

36. Ottardi C, Galbusera F, Luca A, Prosdocimo L, Sasso M, Brayda-Bruno M, et al. Finite element analysis of the lumbar destabilization following pedicle subtraction osteotomy. *Med Eng Phys*. (2016) 38(5):506–9. doi: 10.1016/j.medengphy.2016.02.002

37. Wilson DC, Niosi CA, Zhu QA, Oxland TR, Wilson DR. Accuracy and repeatability of a new method for measuring facet loads in the lumbar spine. *J Biomech*. (2006) 39(2):348–53. doi: 10.1016/j.jbiomech.2004.12.011

38. Renner SM, Natarajan RN, Patwardhan AG, Havey RM, Voronov LI, Guo BY, et al. Novel model to analyze the effect of a large compressive follower pre-load on range of motions in a lumbar spine. *J Biomech*. (2007) 40(6):1326–32. doi: 10.1016/j.jbiomech.2006.05.019

39. Kim HJ, Chun HJ, Moon SH, Kang KT, Kim HS, Park JO, et al. Analysis of biomechanical changes after removal of instrumentation in lumbar arthrodesis by finite element analysis. *Med Biol Eng Comput*. (2010) 48(7):703–9. doi: 10.1007/s11517-010-0621-2

40. Zhao X, Du L, Xie Y, Zhao J. Effect of lumbar lordosis on the adjacent segment in transforaminal lumbar interbody fusion: a finite element analysis. *World Neurosurg*. (2018) 114:e114–20. doi: 10.1016/j.wneu.2018.02.073

41. Polikeit A, Ferguson SJ, Nolte LP, Orr TE. Factors influencing stresses in the lumbar spine after the insertion of intervertebral cages: finite element analysis. *Eur Spine J*. (2003) 12(4):413–20. doi: 10.1007/s00586-002-0505-8

42. Zhong ZM, Deviren V, Tay B, Burch S, Berven SH. Adjacent segment disease after instrumented fusion for adult lumbar spondylolisthesis: incidence and risk factors. *Clin Neurol Neurosurg*. (2017) 156:29–34. doi: 10.1016/j.clineuro.2017.02.020

43. Wilke HJ, Wenger K, Claes L. Testing criteria for spinal implants: recommendations for the standardization of in vitro stability testing of spinal implants. *Eur Spine J*. (1998) 7(2):148–54. doi: 10.1007/s005860050045

44. Chao CK, Hsu CC, Wang JL, Lin J. Increasing bending strength and pullout strength in conical pedicle screws: biomechanical tests and finite element analyses. *J Spinal Disord Tech*. (2008) 21(2):130–8. doi: 10.1097/BSD.0b013e318073cc4b

45. O'Leary SA, Paschos NK, Link JM, Klineberg EO, Hu JC, Athanasiou KA. Facet joints of the spine: structure-function relationships, problems and treatments, and the potential for regeneration. *Annu Rev Biomed Eng*. (2018) 20:145–70. doi: 10.1146/annurev-bioeng-062117-120924

46. O'Leary SA, Link JM, Klineberg EO, Hu JC, Athanasiou KA. Characterization of facet joint cartilage properties in the human and interspecies comparisons. *Acta Biomater*. (2017) 54:367–76. doi: 10.1016/j.actbio.2017.03.017

47. Wang B, Hua W, Ke W, Lu S, Li X, Zeng X, et al. Biomechanical evaluation of transforaminal lumbar interbody fusion and oblique lumbar interbody fusion on the adjacent segment: a finite element analysis. *World Neurosurg*. (2019) 126:e819–24. doi: 10.1016/j.wneu.2019.02.164

48. Liang J, Dong Y, Zhao H. Risk factors for predicting symptomatic adjacent segment degeneration requiring surgery in patients after posterior lumbar fusion. *J Orthop Surg Res*. (2014) 9:97. doi: 10.1186/s13018-014-0097-0

49. Adams MA, Roughley PJ. What is intervertebral disc degeneration, and what causes it? *Spine*. (2006) 31(18):2151–61. doi: 10.1097/01.brs.0000231761.73859.2c

50. Vergroesen PP, Kingma I, Emanuel KS, Hoogendoorn RJ, Welting TJ, van Royen BJ, et al. Mechanics and biology in intervertebral disc degeneration: a vicious circle. *Osteoarthr and Cartil*. (2015) 23(7):1057–70. doi: 10.1016/j.joca.2015.03.028

51. Schmidt H, Galbusera F, Rohlmann A, Shirazi-Adl A. What have we learned from finite element model studies of lumbar intervertebral discs in the past four decades? *J Biomech*. (2013) 46(14):2342–55. doi: 10.1016/j.jbiomech.2013.07.014

52. Pezowicz CA, Schechtman H, Robertson PA, Broom ND. Mechanisms of anular failure resulting from excessive intradiscal pressure: a microstructural-micromechanical investigation. *Spine*. (2006) 31(25):2891–903. doi: 10.1097/01.brs.0000248412.82700.8b

53. Qasim M, Natarajan RN, An HS, Andersson GB. Damage accumulation location under cyclic loading in the lumbar disc shifts from inner annulus lamellae to peripheral annulus with increasing disc degeneration. *J Biomech*. (2014) 47(1):24–31. doi: 10.1016/j.jbiomech.2013.10.032

54. Stefanakis M, Al-Abbasi M, Harding I, Pollintine P, Dolan P, Tarlton J, et al. Annulus fissures are mechanically and chemically conducive to the ingrowth of nerves and blood vessels. *Spine*. (2012) 37(22):1883–91. doi: 10.1097/BRS.0b013e318263ba59

55. García-Cosamalón J, del Valle ME, Calavia MG, García-Suárez O, López-Muñiz A, Otero J, et al. Intervertebral disc, sensory nerves and neurotrophins: who is who in discogenic pain? *J Anat*. (2010) 217(1):1–15. doi: 10.1111/j.1469-7580.2010.01227.x

56. Ravindra VM, Senglaub SS, Rattani A, Dewan MC, Härtl R, Bisson E, et al. Degenerative lumbar spine disease: estimating global incidence and worldwide volume. *Global Spine J*. (2018) 8(8):784–94. doi: 10.1177/2192568218770769

57. Szkoda-Poliszuk K, Żak M, Pezowicz C. Finite element analysis of the influence of three-joint spinal complex on the change of the intervertebral disc bulge and height. *Int J Numer Method Biomed Eng*. (2018) 34(9):e3107. doi: 10.1002/cnm.3107